A Molecular Approach to Apoptosis in the Human Heart During Brain Death

Silvia Pérez López,[1,6] Natalia Vázquez Moreno,[1] Dolores Escudero Augusto,[1,2] Aurora Astudillo González,[3] Francisco Álvarez Menéndez,[4] Félix Goyache Goñi,[5] and Jesús Otero Hernández[1,2]

Background. Brain death induces changes in tissues and organs destined for transplant at the cell, molecular, and endocrine level including cell death through apoptosis. This study was designed to examine apoptotic damage in cardiac tissue obtained from brain dead donors.

Methods. Fifty tissue specimens from the left ventricles of individual donors were processed to evaluate changes in the expression levels of five genes involved in apoptosis (*BAX*, *BCL2*, *CASPASE 3*, *CYTOCHROME C*, and *FAS*) using the real time-polymerase chain reaction technique. Expression levels were quantified by the relative standard method and results normalized to the levels recorded for the endogenous control peptidylprolyl isomerase A. The *HIF1α* gene was also determined to check for the possibility of hypoxic damage. Control ventricular tissue specimens were obtained from patients undergoing mitral valve replacement.

Results. Using a mixed linear model it was determined that the sample type (donor vs. control patient) significantly affected ($P<0.0001$) expression levels of the genes examined reflected by their C_t values. Three of the genes (*BAX*, *CASPASE 3*, and *FAS*) showed significantly higher (Student's t test, $P<0.05$) expression levels (4.89-, 7.85-, and 12.14-fold endogenous control values, respectively) in donors compared with control patients (2.31-, 2.64-, and 3.57-fold endogenous control values, respectively) indicating the activation of apoptosis during brain death.

Conclusion. Our findings suggest the possibility of using antiapoptosis agents to prevent cardiac injury and improve posttransplant behavior.

Keywords: Brain death, Apoptosis genes, Heart transplant, RT-PCR, Organ donor.

(*Transplantation* 2008;86: 977–982)

Brain dead (BD) patients are the main source of organs for transplant. However, in approximately 10%–30% of BD donors, severe myocardial ventricular dysfunction prevents the use of hearts for transplant (*1*), 19% of which are rejected because of contractility failure (*2*). The reason for this situation is related to the hemodynamic and neuroendocrine alterations that appear during cerebral herniation (*3*). Since initial studies performed in experimental models (*4*, *5*), it has been reported that brain death leads to changes that compromise cardiac function. Recently, BD has also been reported to induce apoptosis in animals including the rat (*6*, *7*) and rabbit (*8*) and in several human tissues such as kidney (*9–11*) and heart (*12*). Cardiac apoptosis reduces the contractile mass available, which has been linked to heart failure (*13*). Apoptosis is a cell function necessary for the removal of unwanted cells during normal development or aging. The mechanism is controlled through two major pathways, an extrinsic and intrinsic pathway (*14*), regulated by aspartate-specific cysteine proteases designated caspases (*15*). Activation of the extrinsic pathway makes surface cell death receptors such as Fas bind to their specific ligands (e.g., FasL). The intrinsic pathway is activated by various intracellular stimuli such anoxia or DNA damage, all of which affect mitochondria, where they promote mitochondrial membrane permeabilization and release of caspase activating factors like cytochrome *c* into the cytosol (*16*, *17*). Members of the Bcl-2 family (proapoptotic Bax and antiapoptotic Bcl-2) control activation of the intrinsic path-

---

This research was supported by grant IB05-135 from the FICYT.

Silvia Pérez López performed the RT-PCR experiments and wrote the manuscript. Natalia Vázquez Moreno provided technical assistance. Dolores Escudero Augusto was the main person responsible for obtaining tissue samples from organ donors. Aurora Astudillo González and Francisco Álvarez Menéndez harvested the heart tissue. Félix Goyache Goñi provided statistical analysis assistance and Jesús Otero Hernández designed the project.

The authors have no conflict of interest to declare.

[1] Unidad de Coordinación de Trasplantes y Terapia Celular, Hospital Universitario Central de Asturias, C/Celestino Villamil s/n, Oviedo, Spain.

[2] Servicio de Medicina Intensiva, Hospital Universitario Central de Asturias, C/Celestino Villamil s/n, Oviedo, Spain.

[3] Servicio de Anatomía Patológica, Hospital Universitario Central de Asturias, C/Celestino Villamil s/n, Oviedo, Spain.

[4] Servicio de Bioquímica Clínica, Hospital Universitario Central de Asturias, C/Celestino Villamil s/n, Oviedo, Spain.

[5] Área de Genética y Reproducción Animal, SERIDA-Somió, C/Camino de los Claveles, Gijón, Spain.

[6] Address correspondence to: Silvia Pérez López, Laboratorio de Trasplante y Terapia Celular, Hospital Universitario Central de Asturias, Edificio Polivalente A, 1° planta, C/Celestino Villamil s/n, 33006 Oviedo, Spain.

E-mail: silvia.perez@sespa.princast.es

Received 2 April 2008. Revision requested 30 April 2008.
Accepted 12 June 2008.

ISSN 0041-1337/08/8607-977
DOI: 10.1097/TP.0b013e318186d6d6

way and play an important role in cardiomyocyte apoptosis in rats (*18*). Briefly, for each stimulus, the balance between death and survival seems to be determined by the ratio of apoptosis-stimulating to apoptosis-suppressing Bcl-2 family members (*19*, *20*). Activation of both apoptotic pathways (extrinsic and intrinsic) culminates in the activation of effector caspases (caspase-3, -6, and -7). Effector caspases have many substrates, whose cleavage mediates chromatin condensation and DNA fragmentation as well as the cell morphology changes characteristic of apoptosis (*21*). Activation of the terminal stage of the apoptotic pathway has also been suggested to play an important role (*8*, *22*) in the myocardial dysfunction that appears in grafted hearts from brain-dead donors (*23*, *24*). Given that the process of apoptosis can be pharmaceutically manipulated, the noninvasive identification of apoptosis is critical (*25*). Because apoptosis is a controlled process with different targets for therapeutic intervention (*26*), antiapoptotic treatments could serve to prevent cardiac injury and avoid posttransplant complications. However, little is known about the molecular mechanisms that give rise to cardiac apoptotic alterations induced by BD in humans (*9*, *22*). The aim of this study performed on cardiac tissue from brain-dead donors was to examine through real time-polymerase chain reaction (RT-PCR) the expression of several genes involved in the apoptotic cascade (*BAX*, *BCL2*, *CASPASE 3*, *CYTOCHROME C*, and *FAS*) to determine whether it is activated during BD. To exclude the possibility that our results could be attributable to hypoxia, *HIF1α* gene expression was also determined.

MATERIALS AND METHODS

Sample Collection

Tissue samples were obtained from the left ventricles of 50 heart beating donors (28 men, 22 women; mean age, 61 years; range, 30–80 years). Control samples were heart tissue specimens obtained from the left ventricles of 12 patients (6 men, 6 women; mean age, 65 years; range, 49–83 years) undergoing mitral valve replacement for double mitral lesion. In these patients, left ventricular end-diastolic pressures were moderately elevated over normal levels ≈8±2.2 mm Hg. Samples were obtained over a year, from April 2006 to May 2007. The heart-beating donors had died in a multidisciplinary intensive care unit of a tertiary university hospital. Brain death was attributed to several causes (28 deaths to subarachnoid or intracerebral hemorrhage, 3 to cerebrovascular anoxia, 16 to traumatic brain injury, and 3 to anoxic brain injury). Mean intensive care unit stay before donation was 93 hr (range, 7–624 hr). No donor had previous heart pathology. Consent for organ donation for transplant and clinical research was obtained from the relatives of each donor and control patient.

The donor hearts had been rejected for transplant because of donor age or weight, or recipient blood group incompatibility. The hearts from the 30- to 40-year-old donors that were incompatible with recipients on the Spanish waiting list, had not been accepted as competitive donors elsewhere in Europe. Left ventricular specimens were obtained by the Cavalieri principle of sectioning. After delivering cardioplegia, all cardiac tissues (from donors and controls) were freshly harvested, immediately embedded in O.C.T Compound (Tissue Tek, Sakura, Netherlands) and then stored at −80°C.

RNA Extraction and cDNA Synthesis

Total RNA was isolated using the Nucleo Spin RNA II Isolation Kit (Macherey-Nagel Gmb H & Co. KG) according to the manufacturer's instructions.

The quality of the RNA was assessed through absorbance measurements made using a NanoDrop ND-1000 UV–Vis Spectrophotometer (NanoDropTechnologies, Wilmington, DE). All the samples used in the PCR procedures showed a 260/280 nm absorbance ratio between 1.8 and 2.2. A ratio of approximately 2 is generally accepted as pure for RNA.

Each RNA sample was reverse transcribed using the oligo-pdT and random primers provided in the first-strand complementary DNA (cDNA) synthesis kit for RT-PCR (AMV; Roche Diagnostic, Switzerland) following the manufacturer's instructions. The cDNA samples were then cooled at 4°C and stored at −20°C until use. To confirm the total absence of residual RNA, we performed a conventional PCR on β-actin (GenBank: E00829) (β-actin forward primer 5′-ACTACCTCATGAAGATCCTC-3′; β-actin reverse primer 5′-CGGATGTCCACGTCACACTTC-3′). The PCR protocol consisted of an initial denaturation step at 94°C for 5 min, followed by 35 amplification cycles. Each cycle involved a denaturation step of 30 sec at 94°C, followed by 30 sec of primer annealing at 55°C and 30 sec of primer extension at 72°C, followed by a final extension of 10 min. Amplicon size was confirmed by electrophoresis using an ethidium bromide-stained 2% agarose gel in 1× TBE buffer.

Real-Time Quantitative Polymerase Chain Reaction

The primers for the genes examined were designed using Beacon Designer software (Premier Biosoft International, CA). Table 1 provides the primer sequences and annealing temperatures used.

Quantitative PCR was performed using an i-Cycler iQ Real-Time PCR Detection System (Bio-Rad, Hercules, CA). SYBR Green PCR Supermix (2×) (Bio-Rad), which detects amplification using Sybr Green as a double-stranded DNA-specific fluorescent dye, was used as a mastermix. Assays were performed in duplicate and a blank included in every assay. The reaction mixture for amplification comprised 2 μL of cDNA, 0.4 μL of each primer (forward and reverse primers; final concentration 0.1 μM), 10 μL of Sybr Green mix, and sterile water in a final volume of 20 μL. The RT-PCR protocol included an initial step of 95°C (3 min), followed by 40 cycles of 30 sec at 95°C for DNA denaturation, 40 sec for primer annealing at different temperatures depending on the gene (Table 1), and 40 sec at 72°C for primer extension. Fluorescence data were acquired at 72°C. Melting-curve analysis to confirm product specificity was performed immediately after amplification following 1 min of denaturation at 95°C, 1 min annealing at 65°C, and 60 cycles of 0.5°C increments (10 sec each) beginning at 65°C while monitoring fluorescence. Product identity was confirmed by electrophoresis using an ethidium bromide-stained 2% agarose gel in 1× TBE buffer.

Polymerase chain reaction efficiencies were calculated from a relative standard curve derived from a pool of heart tissue specimens from the same organ donors that was serially

TABLE 1. Genbank accession numbers, annealing temperatures, and primer sequences for the human genes tested by RT-PCR

Gene	Genbank acc. no.	Annealing temperature (°C)	Sequence
BAX	NM138761	60	Forward: 5′ GAT-GCG-TCC-ACC-AAG-AAG-C Reverse: 5′ CCA-GTT-GAA-GTT-GCC-GTC-AG
BCL2	NM004049	57	Forward: 5′ GAT-GCG-TCC-ACC-AAG-AAG-C Reverse: 5′ CCA-GTT-GAA-GTT-GCC-GTC-AG
CASPASE 3	NM032991	57	Forward: 5′ CTG-GAC-TGT-GGC-ATT-GAG-AC Reverse: 5′ ACA-AAG-CGA-CTG-GAT-GAA-CC
CYT C	NM018947	60	Forward: 5′ TGG-GTG-ATG-TTG-AGA-AAG-G Reverse: 5′ CGG-CTG-TGT-AAG-AGT-ATC-C
FAS	NM000043	57	Forward: 5′ CGT-CTG-TTG-CTA-GAT-TAT-CG Reverse: 5′ TTG-TCT-GTG-TAC-TCC-TTC-C
HIF1α	NM001530	58	Forward: 5′ GAA-GAC-ACA-GAA-GCA-AAG-AAC-C Reverse: 5′ GTG-GTA-GTG-GTG-GCA-TTA-GC

Table provides the accession numbers for the six genes examined: the antiapoptotic and apoptotic genes *BAX*, *BCL2*, *CASPASE 3*, *CYTOCHROME C*, and *FAS* and the gene *HIF1α* as an indicator of hypoxic damage. All primer sequences were designed using Beacon Designer software.

CYT C, Cytochrome C; RT-PCR, real-time polymerase chain reaction.

diluted (a 10-fold dilution series with at least six measuring points). Peptidylprolyl isomerase A (cyclophilin A) was used as the endogenous control (Human Endogenous Control Gene Panel, TATAA Biocenter, Goteborg, Sweden) according to the manufacturer's instructions.

Statistical Analysis

Data were statistically analyzed using the Proc MIXED procedure of the SAS/STAT v8.2 software package (SAS Institute, Inc., Cary, NC). C_t values (number of cycles needed to generate a fluorescent signal above a predefined threshold) and ΔC_t values (difference between the C_t of the target gene and that of the housekeeping gene) for each gene and repetition were used as dependent variables. The relative standard method was used to quantify gene expression levels.

The model fitted included the type of sample (two levels: control vs. donor) as the fixed effect, and the sample as a random effect to account for the nonindependency of repetitions. Least-square means and their corresponding standard errors were computed for each sample level. For descriptive purposes, a Student's *t* test was also carried out on raw C_t means computed for control and donor samples using Proc GLM of SAS/STAT, assuming that the sample type effect included two independent groups of normally distributed observations. Correlation coefficients between levels of expression were computed using the Proc CORR implemented in SAS/STAT.

RESULTS

Product identity was confirmed by electrophoresis on ethidium bromide-stained 2% agarose gels in 1× TBE buffer, which resulted in a single product of the desired length. In addition an i-Cycler iQ melting curve analysis was performed, which rendered single product specific melting temperatures. No primer-dimers were generated during the 40 real-time PCR cycles conducted (see Table 2).

TABLE 2. Amplicon size and melting temperatures of the six genes analyzed by RT-PCR

Genes	Amplicon size (bp)	Melting temperature (°C)
BAX	165	86
BCL2	165	86.5
CASPASE3	159	83
CYT C	153	84.5
FAS	244	85
HIF1α	230	82.5

Product identity was confirmed by electrophoresis, which resulted in a single product of the desired length. Melting curve analysis was also performed, rendering in each case a single product-specific melting temperature.

CYT C, Cytochrome C; RT-PCR, real-time polymerase chain reaction; bp, base pair.

Polymerase chain reaction efficiencies were 91.7% for *BAX*, 101.5% for *BCL2*, 94.3% for *CASPASE 3*, 101.1% for *CYTOCHROME C*, 94.7% for *FAS*, and 103.2% for *HIF1α*. Linearity was high, with correlation coefficients (R^2) above 0.989.

To confirm the accuracy and reproducibility of real-time PCR, intra-assay precision was determined in two replicates within a single i-Cycler iQ run. Interassay variation was determined in two experimental runs performed on different days. The reproducibility of the data ranged from 95% for *FAS* to 98.8% for *CASPASE* 3 and *CYTOCHROME C*.

Gene Expression

The mixed linear model indicated a significant influence of the type of sample (donor vs. control) on C_t values at *P* less than 0.0001. The Student's *t* test computed on raw means also revealed that differences between the type of sample were significant at the level *P* less than 0.05 for all the genes examined. Least-square C_t means and their corresponding standard errors for each gene according to the sample type (control or donor) are given in Table 3.

To quantify gene expression, the relative standard method (relative fold changes) was used and expression levels

TABLE 3. C_t (threshold cycle) values for the two study groups (brain-dead donors vs. control patients) represented as Lsmean and SEM

Gene	Sample	Lsmean	SEM
BAX	Control	35.1367	0.5584
	Donor	31.6283	0.2681
BCL2	Control	34.6723	0.5972
	Donor	31.5346	0.2745
CASPASE 3	Control	33.445	0.6682
	Donor	29.4894	0.3073
CYT C	Control	25.8755	0.5179
	Donor	23.1565	0.2382
FAS	Control	34.3758	0.9349
	Donor	30.1238	0.3946
HIF1α	Control	33.6809	0.5918
	Donor	31.0102	0.2776

Significant differences between the donor (n=50) and control (n=12) specimens ($P<0.05$) were recorded for all the genes examined (Student's *t* test).

CYT C, Cytochrome C; SEM, standard error of mean; Lsmean, least-square C_t means.

determined for the donor and control groups normalized to the level for peptidylprolyl isomerase A (*PPIA*). A marked increase was noted in the relative expression of three of the genes in the donor compared with control heart tissue specimens. These increases are plotted in Figure 1. In the heart-beating donor group, the genes *FAS*, *CASPASE 3*, and *BAX* were up-regulated 12.14-, 7.85-, and 4.89-fold, respectively, with respect to the basal levels recorded for the endogenous control (*PPIA*). For the same three genes increases in control group specimens were 3.57-, 2.64-, and 2.31-fold, respectively, over basal levels. Differences in expression level increases were significant between the donor and control groups.

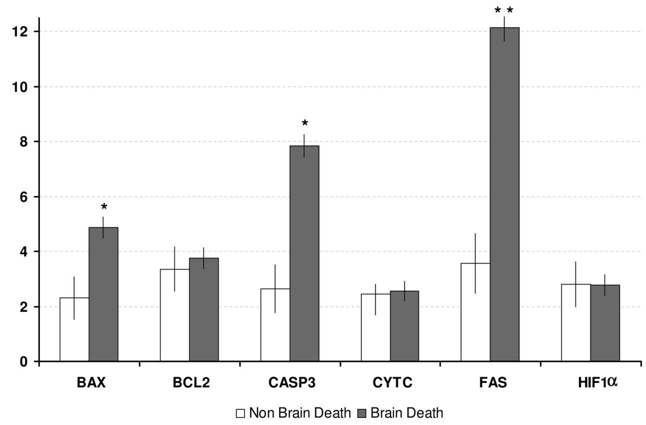

FIGURE 1. Relative quantification of the studied genes. mRNA levels for apoptosis-related genes recorded in the heart tissue of brain-dead (BD) donors (n=50) and control patients (n=12) relative to levels for the endogenous control gene peptidylprolyl isomerase A. Values are expressed as mean±SEM. * indicates a significant difference compared with controls at *P* less than 0.05. ** indicates a significant difference between the two groups at *P* less than 0.01. *CYT C*, cytochrome C; *Casp3*, Caspase 3.

The remaining genes showed less pronounced increases in expression levels. In descending order, these increments were 3.76-fold for the *BCL2* gene, 2.78-fold for *HIF1α*, and 2.56-fold for *CYTOCHROME C* compared with basal levels. Increases for the control group were 3.36-, 2.80-, and 2.45-fold, respectively. This time, differences between the control and donor groups were not significant.

Correlation coefficients among expression levels of the six genes in all the samples examined are provided in Table 4. All the computed correlation coefficients were significant at a $P<0.0001$ and ranged from moderate (0.395 for *HIF1α-FAS*) to high (0.852 for *BAX-CYTC*).

DISCUSSION

Current estimates of the proportion of hearts rejected for transplant because of ventricular dysfunction range from 10% (*27*) to 30% (*1*). Of these, 19% have contractility problems (*1*) and are therefore not suitable for transplant purposes. Several authors have recently observed an active apoptotic process during BD (*9*, *10*). The time taken from the initiation of the apoptotic process to phagocytosis of the dying cell is unknown, but estimates range from hours to days (*28*), a time interval that basically coincides with the death of brain-dead donors. Cardiac myocyte apoptosis occurs in several human heart diseases such as congestive heart failure (*29*, *30*) or arrhythmogenic ventricular dysplasia (*31*) or myocarditis (*32*). If the apoptotic process is really activated during BD, this could lead to a substantial loss of contractile mass possibly accounting for the percentage of donor hearts with compromised contractility. In this study, we used a molecular approach to assess how the BD phenomenon affects human cardiac tissue in the damage sustained through apoptosis by detecting differences in the levels of expression of six different genes (*BAX*, *BCL2*, *CASPASE 3*, *CYTOCHROME C*, *FAS*, and *HIF1α*) using the *PPIA* gene to normalize the data (*33*) in a relative RT-PCR quantification procedure.

To establish whether apoptosis is indeed in an active mechanism in heart tissue during brain death, we examined several genes involved in the intrinsic and extrinsic apoptotic pathway. CASPASE 3 represents the final common pathway of the apoptotic cascade (*34*) and has been identified in neonatal (*35*) and adult rat cardiomyocytes (*36*). In our cardiac

TABLE 4. Intergene correlation analysis of q-PCR expression levels

	BAX	CYTC	HIF1α	BCL2	FAS
CYTC	0.85273				
HIF1α	0.74487	0.75717			
BCL2	0.66986	0.6507	0.68568		
FAS	0.49237	0.41556	0.39509	0.60124	
Casp3	0.65702	0.56326	0.6016	0.73148	0.58561

All the computed correlation coefficients (R^2) for the six genes were significant at *P* less than 0.0001. All pair-wise correlation coefficients were calculated on qPCR expression levels remaining after normalization with values obtained for the endogenous control PPIA (cyclophilin A).

CYT C, Cytochrome C; *Casp3*, Caspase 3; *PPIA*, peptidylprolyl isomerase A.

specimens from brain-dead donors, *CASPASE 3* expression levels were 7.85-fold higher than basal levels and, remarkably, this increase differed significantly ($P<0.05$) from that recorded for the control cardiac specimens. We also examined expression levels of the *FAS* gene. FAS is a cell death receptor that belongs to the TNFR gene superfamily (*37*) with a role in activation of the extrinsic pathway. Our results indicate elevated expression levels of this gene by as much as 12.14-fold basal levels in heart tissue from heart beating donors, this increase being significantly greater than that detected in controls ($P<0.01$). Further apoptotic molecules determined here were *BCL2* and *BAX* (members of the apoptosis-stimulating and suppressing Bcl-2 family). These molecules underwent 3.76- and 4.89-fold increases, respectively, over basal levels such that the ratio of *BAX* (proapoptotic)-to-*BCL2* (antiapoptotic) expression was clearly in favor of the apoptotic molecule. These two molecules have been described to indicate the balance between cell death and survival (*38*). Finally, to complete our molecular approach to apoptosis we analyzed expression of the *CYTOCHROME C* gene. The release of this molecule and other mitochondrial proapoptotic factors into the cytosol (*39*) is induced by proapoptotic family members such as BAX as part of the intrinsic pathway. We observed no significant difference in the expression of this gene between the two groups of cardiac specimens. Because hypoxia can stimulate components of cell death receptor and mitochondrial pathways (*40*) and cardiac myocyte apoptosis has been induced by hypoxia in rats (*41*), we also examined the gene (*HIF1α*) to rule out the possibility that our results could be caused by hypoxia. Hypoxia-inducible factor 1 (HIF1α) is a heterodimeric transcription factor consisting of an oxygen-regulated alpha subunit and a constitutively expressed beta subunit. HIF1α protein has been detected in distinct cell types in vivo and its expression is increased in response to hypoxia (*42*). We observed low-*HIF1α* expression levels in control and donor specimens such that we can preclude any major hypoxic damage to the heart tissue immediately after harvesting and, surprisingly, neither did there seem to be a marked difference in the hypoxia suffered by the two sources of heart tissue. Our results are in agreement with a report (*43*) that hypoxia seems not to be one of the starting points for the inflammatory cascade in brain-dead donor kidneys. In a molecular study performed on the liver of heart beating rats (*6*), apoptotic genes such as *FAS*, *BAX*, or *CASPASE 3* increased their expression levels versus controls as a consequence of BD. Our data indicate a marked increase in the expression of three of the genes examined (*BAX*, *CASPASE 3*, and *FAS*) compared with controls. If we consider that each of these genes play a different role in the apoptotic process (*BAX* participates in the intrinsic pathway, *FAS* in the extrinsic pathway, and *CASPASE* 3 is an effector caspase), we could say that our results suggest that although both apoptotic pathways were active, the intrinsic pathway was activated to a much lesser extent than the extrinsic. Given that one of the main stimuli that activates the intrinsic pathway is anoxia, the lack of substantial increases in the expression levels of the gene related to hypoxia (*HIF1α*) and those involved in the intrinsic pathway (*BAX* or *CYTOCHROME C*) are consistent with our findings. In conclusion, our results suggest that the apoptotic process is initiated during brain death in cardiac tissue from heart beating donors. If these results are confirmed, they suggest the possible use of antiapoptotic treatments to prevent organ damage before transplantation.

ACKNOWLEDGMENTS

The authors thank Dr. Valle Castro for his help in obtaining the control tissue specimens and Benjamin Otero and Pilar Alonso for help with the donor tissue specimens.

REFERENCES

1. Chamorro C, Romera MA, Silva JA, et al. Can heart donation exclusion factors be overcome? *Rev Esp Cardiol* 2006; 59: 232.
2. Gallardo A, Anguita M, Franco M, et al. The echocardiographic findings in patients with brain death, the implications for their selection as heart transplant donors. *Rev Esp Cardiol* 1994; 47: 604.
3. Owen VJ, Burton PBJ, Michel MC, et al. Myocardial dysfunction in donor hearts. A possible etiology. *Circulation* 1999; 99: 2565.
4. Cooper DK, Novitzky D, Wicomb WN. The pathophysiological effects of brain death on potential donor organs, with particular reference to the heart. *Ann R Coll Surg Engl* 1989; 71: 261.
5. Novitzky D, Horak A, Cooper DK, et al. Electrocardiographic and histopathologic changes developing during experimental brain death in the baboon. *Transplant Proc* 1989; 21(1 Pt 3): 2567.
6. Van Der Hoeven JA, Moshage H, Schuurs T, et al. Brain death induces apoptosis in donor liver of the rat. *Transplantation* 2003; 76: 1150.
7. Kusaka M, Fukami N, Sasaki H, et al. IP-10, apoptotic genes, and calcineurin subtype messenger RNA kinetics occurring in rat renal isografts from brain-dead donors. *Transplant Proc* 2005; 37: 361.
8. Kirsch M, Bertrand S, Lecerf L, et al. Brain death-induced myocardial dysfunction: A role for apoptosis? *Transplant Proc* 1999; 31: 1713.
9. Carstens J, Markussen N, Madsen M. The granule exocytosis and Fas/FasLigand pathways at the time of transplantation and during borderline and acute rejection of human renal allografts. *Transplant Proc* 2005; 37: 3294.
10. Hes O, Treska V, Hasman D, et al. Determination of apoptotic cells in kidneys from non-heart-beating donors and heart-beating donors using the TUNEL assay: A limited immunohistochemical method? *Transplant Proc* 2002; 34: 1095.
11. Nijboer WN, Schuurs TA, van der Hoeven JA, et al. Effect of brain death on gene expression and tissue activation in human donor kidneys. *Transplantation* 2004; 78: 978.
12. Yeh T Jr, Wechsler AS, Graham LJ, et al. Acute brain death alters left ventricular myocardial gene expression. *J Thorac Cardiovasc Surg* 1999; 117: 365.
13. Khoynezhad A, Jalali Z, Tortolani AJ. A synopsis of research in cardiac apoptosis and its application to congestive heart failure [review]. *Tex Heart Inst J* 2007; 34: 352.
14. Budihardjo I, Oliver H, Lutter M, et al. Biochemical pathways of caspase activation during apoptosis. *Annu Rev Cell Dev Biol* 1999; 15: 269.
15. Patel T, Gores GJ, Kaufmann SH. The role of proteases during apoptosis [review]. *FASEB J* 1996; 10: 587.
16. Saikumar P, Venkatachalam MA. Role of apoptosis in hypoxicischemic damage in the kidney. *Semin Nephrol* 2003; 23: 511.
17. Kroemer G, Reed JC. Mitochondrial control of cell death. *Nat Med* 2000; 6: 513.
18. Kunisada K, Tone E, Negoro S, et al. Bcl-xl reduces doxorubicin-induced myocardial damage but fails to control cardiac gene downregulation. *Cardiovasc Res* 2002; 53: 936.
19. Saikumar P, Dong Z, Mikhailov V, et al. Apoptosis: Definition, mechanisms, and relevance to disease. *Am J Med* 1999; 107: 489.
20. Antonsson B. Bax and other pro-apoptotic Bcl-2 family "killer-proteins" and their victim the mitochondrion. *Cell Tissue Res* 2001; 306: 347.
21. Thornberry NA, Lazebnik Y. Caspases: Enemies within. *Science* 1998; 281: 1312.
22. Birks EJ, Yacoub MH, Burton PS, et al. Activation of apoptotic and inflammatory pathways in dysfunctional donor hearts. *Transplantation* 2000; 70: 1498.
23. Laguens RP, Meckert PM, Martino JS, et al. Identification of programmed cell death (apoptosis) in situ by means of specific labeling of nuclear DNA fragments in heart biopsy samples during acute rejection episodes. *J Heart Lung Transplant* 1996; 15: 911.

24. Szabolcs MJ, Ravalli S, Minanov O, et al. Apoptosis and increased expression of inducible nitric oxide synthase in human allograft rejection. *Transplantation* 1998; 65: 804.
25. Puig M, Ballester M, Matías-Guiu X, et al. Burden of myocardial damage in cardiac allograft rejection: Scintigraphic evidence of myocardial injury and histologic evidence of myocyte necrosis and apoptosis. *J Nucl Cardiol* 2000; 7: 132.
26. Reeve JL, Duffy AM, O'Brien T, et al. Don't lose heart–Therapeutic value of apoptosis prevention in the treatment of cardiovascular disease. *J Cell Mol Med* 2005; 9: 609.
27. Gilbert EM, Krueger SK, Murray JL, et al. Echocardiographic evaluation of potential cardiac transplant donors. *J Thorac Cardiovasc Surg* 1988; 95: 1003.
28. Cook SA, Poole-Wilson PA. Cardiac myocyte apoptosis [review]. *Eur Heart J* 1999; 20: 1619.
29. Olivetti G, Abbi R, Quaini F, et al. Apoptosis in the failing human heart. *N Engl J Med* 1997; 336: 1131.
30. Narula J, Haider N, Virmani R, et al. Apoptosis in myocytes in end-stage heart failure. *N Engl J Med* 1996; 335: 1182.
31. Mallat Z, Tedgui A, Fontaliran F, et al. Evidence of apoptosis in arrhythmogenic right ventricular dysplasia. *N Engl J Med* 1996; 335: 1190.
32. Toyozaki T, Hiroe M, Tanaka M, et al. Levels of soluble Fas ligand in myocarditis. *Am J Cardiol* 1998; 82: 246.
33. Pérez S, Royo LJ, Astudillo A, et al. Identifying the most suitable endogenous control for determining gene expression in hearts from organ donors. *BMC Mol Biol* 2007; 8: 114.
34. Earnshaw WC, Martins LM, Kaufmann SH. Mammalian caspases: Structure, activation, substrates, and functions during apoptosis [review]. *Annu Rev Biochem* 1999; 68: 383.
35. Yue TL, Wang C, Romanic AM, et al. Staurosporine-induced apoptosis in cardiomyocytes: A potential role of caspase-3. *J Mol Cell Cardiol* 1998; 30: 495.
36. Black SC, Huang JQ, Rezaiefar P, et al. Co-localization of the cysteine protease caspase-3 with apoptotic myocytes after in vivo myocardial ischemia and reperfusion in the rat. *J Mol Cell Cardiol* 1998; 30: 733.
37. Ashkenazi A. Targeting death and decoy receptors of the tumour-necrosis factor superfamily [review]. *Nat Rev Cancer* 2002; 2: 420.
38. Adams JM, Cory S. The Bcl-2 protein family: Arbiters of cell survival [review]. *Science* 1998; 281: 1322.
39. Luo X, Budihardjo I, Zou H, et al. Bid, a Bcl2 interacting protein, mediates cytochrome c release from mitochondria in response to activation of cell surface death receptors. *Cell* 1998; 94: 481.
40. Reeve JL, Szegezdi E, Logue SE, et al. Distinct mechanisms of cardiomyocyte apoptosis induced by doxorubicin and hypoxia converge on mitochondria and are inhibited by Bcl-xL. *J Cell Mol Med* 2007; 11: 509.
41. Tanaka M, Ito H, Adachi S, et al. Hypoxia induces apoptosis with enhanced expression of Fas antigen messenger RNA in cultured neonatal rat cardiomyocytes. *Circ Res* 1994; 75: 426.
42. Stroka DM, Burkhardt T, Desbaillets I, et al. HIF-1 is expressed in normoxic tissue and displays an organ-specific regulation under systemic hypoxia. *FASEB J* 2001; 15: 2445.
43. Schuurs TA, Morariu AM, Ottens PJ, et al. Time-dependent changes in donor brain death related processes. *Am J Transplant* 2006; 6: 2903.